

# A First Measurement Study of Commercial mmWave 5G Performance on Smartphones

Arvind Narayanan, Jason Carpenter, Eman Ramadan,  
 Qingxu Liu, Yu Liu, Feng Qian, Zhi-Li Zhang  
 University of Minnesota – Twin Cities

**Abstract.** We conduct to our knowledge a first measurement study of commercial mmWave 5G performance on smartphones by closely examining 5G networks in two U.S. cities. We conduct extensive field tests on 5G performance under diverse conditions including different obstruction levels, phone-tower distances, and device orientations. We systematically analyze the handoff mechanisms in 5G and their impact on network performance. We also study app performance (web browsing and HTTP download) over 5G, and how Internet server selection affects the end-to-end performance for 5G users. Our experiments consume 10 TB of 5G data, conducted when 5G just made its debut in April 2019. These experiments provide a “baseline” for studying how 5G performance evolves, and identify key research directions on improving 5G users’ experience in a cross-layer manner.

## 1 INTRODUCTION

2019 marks the year for 5G, which was eventually rolled out for commercial services to consumers. Compared to 4G LTE, 5G offers significantly higher bandwidth, lower latency, and better scalability (*i.e.*, supporting more devices). The mainstream 5G deployment employs the millimeter wave (mmWave) technology that can provide, in theory, a throughput of up to 20 Gbps – a 100× improvement compared to today’s 4G, as well as <1ms latency [29]. Under the hood, this is achieved by a series of innovations including massive MIMO, advanced channel coding, and scalable modulation.

5G is expected to fuel a wide range of applications that cannot be well supported by 4G, such as ultra-HD (UHD) video streaming, networked VR/AR, low-latency cloud gaming, IoT, and vehicle-to-everything (V2X) communication. Despite these potentials, commercial 5G services are at their infancy. In April 2019, **Verizon** launched 5G in Chicago and Minneapolis. It uses a 400 MHz channel at 28 GHz, making it the world’s first commercial mmWave 5G service for consumers. Most major carriers around the world are rolling out 5G this year or in the process of expanding their footprint to more cities.

In this paper, we conduct to our knowledge a first measurement study of commercial mmWave 5G networks on smartphones. We travel to **Verizon**’s 5G coverage areas at the two cities and conduct detailed measurements of **Verizon**’s

mmWave 5G networks. We compare the performance of 5G and 4G on key metrics such as throughput, latency, and packet loss rate. Since mmWave signals are vulnerable to obstruction and attenuation, we conduct our experiments under diverse scenarios with different distances/orientations between the smartphone and the 5G-NR (New Radio) panel, and obstruction levels. Furthermore, we study other important aspects such as 4G/5G handoffs, application performance, and many of whose characteristics are quite different from those of 4G. Our two-month experiments consume 10 TB 5G traffic and 1 TB 4G traffic<sup>1</sup>. We summarize our key findings as follows.

- 5G offers much higher throughput than 4G (median throughput: 1520 vs. 147 Mbps). However, even under clear line-of-sight, 5G throughput exhibits much higher variation than 4G, mainly due to the PHY-layer nature of 5G signals (§4.1).
- **Verizon** very likely imposes a per-TCP-connection throttling on 5G traffic. This may hurt the performance of single-connection protocols such as HTTP/2. Due to its non-standalone deployment (§2), **Verizon**’s 5G offers little improvement of the end-to-end PING RTT over 4G. However, the bufferbloat becomes less severe likely because of 5G’s high speed (§4.1).
- 5G performance may be affected by obstruction, distance, and device-tower orientation. Among these factors, obstruction typically incurs the highest impact. We find that 5G signals can be easily blocked by hands and human body. Despite that, in urban environments, surrounding signal reflections can oftentimes mitigate the performance degradation, allowing 5G to function under non-line-of-sight (§4.2).
- 4G-5G handoffs can be triggered by either network condition change or user traffic. Even under low mobility (*e.g.*, walking), a smartphone may experience 31 4G/5G handoffs in less than 8 minutes. Due to the discrepancy between 4G and 5G, frequently switching between them may confuse applications (*e.g.*, video rate adaptation logic) and bring highly inconsistent user experiences (§4.3).
- For web browsing, 5G brings little page load time reduction for most small web pages compared to 4G. For large HTTP(S)

<sup>1</sup>We purchased multiple unlimited 5G data plans from **Verizon** for this study. Our study conforms to **Verizon**’s wireless customer agreement.

download, the goodput is significantly lower than the available 5G bandwidth, because many cross-layer factors may potentially slow down the download (§4.4).

At a high level, we find that despite its high throughput, today’s 5G has several limitations such as large performance variations, vulnerability to obstructions, and frequent hand-offs even during low mobility. We also experimentally show that 5G’s high throughput does not always translate to better app QoE, whose improvement requires joint, cross-layer optimizations from multiple players in the mobile ecosystem. We make the following contributions in this paper.

- We develop practical and sound measurement methodologies for mmWave 5G networks on COTS smartphones.
- We present timely measurement findings of mmWave 5G performance on smartphones with key insights. As our experiments were conducted when commercial 5G had just made its debut, our results provide an important “baseline” for studying how 5G performance evolves.
- We intend to release our measurement data to the research community to benefit work that needs real 5G data.

## 2 BACKGROUND AND RELATED WORK

**mmWave** is an innovative technology integrated into 5G. Unlike 3G/4G that works at  $\leq 5$  GHz, mmWave radios operate at much higher frequencies of 30 to 300 GHz. Despite its high bandwidth, mmWave’s short wavelength makes its signals vulnerable to attenuation. To overcome this, mmWave transceivers have to use phased-array antennas to form highly directional beams. Due to the pseudo-optical nature of a beam, the signals are sensitive to blockages such as a pedestrian or a moving vehicle. Switching from line-of-sight (LoS) to none-line-of-sight (NLoS) due to blockage may cause significant data rate drop or even complete blackout despite the beamforming algorithm that attempts to “recalibrate” the beams by seeking for a reflective NLoS path [26, 36].

Researchers have demonstrated the feasibility of deploying mmWave in data centers [12, 44, 46], indoor [1, 2, 5, 11, 25, 37, 39, 41], and outdoor environments [28, 31–33, 43, 45], as well as have conducted many studies on beamforming and beam tracking [8, 27, 34]. But none of them studies mmWave in commercial 5G context on smartphones.

**5G Infrastructure.** To reduce the time to market, carriers may couple their 5G core network equipment with existing 4G LTE infrastructures in what is known as a Non-Standalone Deployment (NSA). NSA utilizes 5G-NR for data plane operations while retaining the 4G infrastructure for control plane operations [14]. NSA is contrasted with a Standalone deployment (SA), which is fully independent of legacy cellular infrastructures. **Verizon**’s 5G uses the NSA model.

**Measurements of Cellular Networks.** There exist a plethora of work on cellular network measurement, such

as crowd-sourced measurements of 3G [16, 35], LTE performance characterization using ISP data [15], studies of cellular network configurations [6], cellular performance under high mobility [20], using cellular to support emerging applications such as VR [38], and measurement tools [21], to name just a few. None of the above work studies 5G networks that have been very recently commercialized.

## 3 MEASUREMENT METHODOLOGY

**5G Networks.** All our experiments were conducted over **Verizon**’s 5G network. As of June 2019, **Verizon** is the only cellular carrier in the U.S. that offers commercial mmWave-based 5G services to consumers at specific downtown areas in two cities: Minneapolis and Chicago. In both cities’ 5G coverage areas, dense 5G base stations are deployed. Due to **Verizon**’s adoption of NSA (§2), 5G base stations are typically co-located with or very close to those of 4G (based on our knowledge and visual inspection). A 5G base station is typically equipped with two *panels* that are the mmWave transceivers. We observe that the panels typically face populated areas such as streets and pedestrian walkways.

**5G User Equipment (UE).** We use two types of COTS 5G-capable smartphones: Motorola Moto Z3 and Samsung Galaxy S10 5G (SM-G977U), henceforth referred to as MZ3 and SGS10, respectively. They are the only two types of commercially available 5G smartphones from **Verizon** as of mid-June 2019. SGS10 has a built-in 5G radio, while MZ3 requires a separate accessory called 5G Mod [23] for accessing 5G. Comparing their performance at same locations, we find that MZ3 significantly underperforms SGS10 in terms of 5G throughput, likely due to hardware issues of MZ3 or its 5G mod. To further ensure that our experiments are not affected by device artifacts, we purchase two SGS10 and confirm that they exhibit similar 5G performance. Our experience indicates the importance of selecting proper devices for studying emerging wireless technologies such as 5G. Thus, unless otherwise mentioned, all 5G results presented in the paper are from SGS10. We confirm that despite 5G’s high throughput, the device-side processing is not a bottleneck. In some experiments, we also employ a Samsung Galaxy S9 (SGS9) over 4G for 4G-5G comparison. We use SGS9 because we are not able to manually switch between 5G and 4G on SGS10.

**Experiment Sites.** We conduct experiments at 4 locations (A, B, C, and D). A is a popular downtown area in Minneapolis with many buildings. B is at the boundary of the 5G coverage area in downtown Minneapolis. C is inside a hotel room in downtown Chicago where we stand near an open window. D is near the U.S. bank stadium in Minneapolis with large open space. We believe that these 4 locations are representative in terms of their environment (open/crowded space, low/high surrounding buildings, indoor/outdoor, *etc.*).

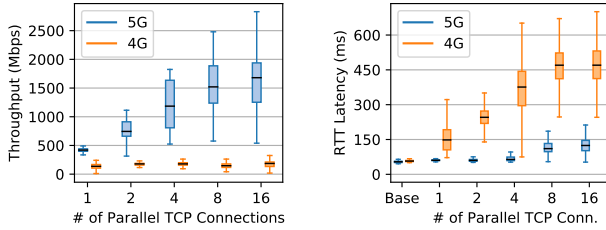


Figure 1: TCP perf. under LoS. (a) throughput, (b) RTT.

**Server Selection.** Due to the ultra-high bandwidth of 5G, the bottleneck of an end-to-end path may easily shift from the wireless hop to the Internet – a situation that seldom appears in 3G/4G. Since the focus of our study is 5G, in most experiments we do *not* want such a shift to occur. To ensure this, we carefully select a Microsoft Azure server located in the U.S. east coast. We justify our selection as follows. First, when downloading data from this server, we get the highest 5G throughput (statistically) compared to servers in other locations or of other cloud providers. Second, when we conduct download test from this server to other hosts (*e.g.*, an Amazon cloud instance) over the Internet, we get  $\sim 3$  Gbps throughput, which is much higher than the highest 5G speed we can obtain, during different times of a day. Based on the above observations, we have high confidence that for an end-to-end path from a UE to our selected server, the Internet is unlikely to become the bottleneck. We also measure how end-to-end performance (latency and HTTP download time) is affected by server selection in §4.1 and §4.4.

**Test Workload.** For most of our experiments, we perform large bulk data transfers for bandwidth probing. Specifically, our UE issues one or more TCP connections or a UDP session to download data from an Internet server. Since it is difficult to root our UEs, we run the cross-compiled version of **iPerf** 3.6 [19] to measure key metrics including throughput, RTT, and packet loss rate. We also experiment with two important applications: web browsing and HTTP(S) file download over 5G, with details to be described in §4.4.

**UE-side 5G Monitoring Tool.** Due to 5G’s very recent debut, we are not aware of any dedicated UE-side monitoring tool for it. We therefore develop one that collects the following information to support our measurements: (1) the UE’s fine-grained location, (2) all available network interfaces, (3) the actively used network interface and its IP address, (4) the cell ID (mCID) that the device is connected to, (5) the cellular signal strength, and (6) the 5G service status. The above information is obtained from Android APIs. Regarding the last item (the 5G service status), we find that when the UE is connected to 5G, it will be in one of three states: (1) the UE is not in 5G coverage area, (2) the UE is in 5G area but is connected to 4G due to, for example, poor 5G signals, and

(3) the UE is connected to 5G. This information is used for the handoff analysis in §4.3.

## 4 MEASUREMENT RESULTS

We now describe our measurement results to highlight TCP performance using 5G, the impact of the environment such as obstruction on 5G, explain 5G handoffs, and finally show the impact of using 5G on application performance.

### 4.1 TCP Performance Under LoS

We begin with understanding 5G performance when clear LoS is present. Specifically, we conduct experiments at Locations A, B, and C (§3). At all locations, we ensure that we can visually see the 5G panel and there is LoS between the phone and the panel. At A and B, we select 5 UE-panel distances from 13m to 75m (we use a laser distance meter [7] to accurately measure the distance). For each distance, we experiment with 3 orientations:  $0^\circ$ ,  $45^\circ$ , and  $90^\circ$  (see Figure 2). For C, the distance (62m) and orientation ( $0^\circ$ ) are fixed.

In each test, we perform TCP bulk download for 60 seconds using  $\{1, 2, 4, 8, 16\}$  parallel TCP connections, and measure the throughput and RTT every second (reported by **iPerf**). For all bulk download tests, unless otherwise mentioned, we start collecting data 20 seconds after the TCP flow(s) start in order to mitigate the impact of TCP slow start. We repeat the entire process 3 times. All experiments were conducted in clear weather with the phone being held in hand. We believe that the above combinations provide realistic and diverse environmental configurations of urban 5G access from smartphones. In addition, during all experiments, we place next to the SGS10 an SGS9 phone to conduct the same tests over 4G. We confirm that between the two phones, there is no interference that may degrade the performance.

The two plots in Figure 1 show the measurement results of throughput and RTT, respectively, for different numbers of concurrent TCP connections. Each boxplot is across all 1-second measurement samples for a specific setup. We make several observations. First, 5G offers much higher throughput than 4G. With 8 parallel TCP connections, the median 5G and 4G throughputs are 1520 and 147 Mbps, respectively. However, 5G throughput exhibits much higher variations than 4G despite the presence of LoS. This is due to the PHY-layer nature of 5G signals as well as potential inefficiencies at various layers. For example, at PHY/MAC layers, smartphones’ small form factor makes engineering 5G modem challenging [30]. At the transport layer, an excessive number of TCP connections may incur cross-connection contentions.

Second, 5G throughput improves as the TCP concurrency level increases. Through controlled experiments over wired networks and WiFi, we confirm that this is not caused by TCP

	First Hop RTT (ms)	East US Total RTT	West US Total RTT
5G	27±6.4	54±4.5	81±5.5
4G	29±4.8	58±4.3	88±5.5

**Table 1: 1st Hop RTT and impact of server’s network location on total (end-to-end) PING RTT on 4G/5G. The reported numbers are averaged across all runs.**

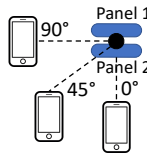


**Figure 2: Orientation.**

itself. We instead believe that **Verizon** is imposing *per-TCP-connection rate limiting* over 5G, whose bandwidth appears to be fully utilized when there are more than 8 concurrent connections. This practice may hurt the performance of single-connection protocols such as HTTP/2 [3].

Third, regarding the latency, 5G and 4G exhibit similar base RTT (*i.e.*, end-to-end PING) at around 56 ms. To understand how much 5G contributes to this RTT, we perform **traceroute** on the UE to measure the hop-by-hop RTT. As shown in Table 1, we find that the first hop RTT, which presumably covers the RAN (Radio Access Network), is around 28 ms for both 4G and 5G, accounting for around 50% of the end-to-end RTT. Changing the server location to west U.S. reduces this fraction to around 33%. Overall, likely due to its NSA model that shares much 4G infrastructure with 5G, **Verizon**’s 5G network provides little improvement of the base RTT over 4G. We expect this to be addressed by the SA model that may achieve the goal of sub-millisecond RTT.

We then consider the RTT during a bulk transfer. As shown in Figure 1(b), 4G RTT inflates drastically because of its deep in-network buffers [15, 17]. Bufferbloat in 5G is much less severe, likely due to the fast 5G speed that drains the buffer much faster than 4G. Also, 5G exhibits low packet loss rates (50%, 75%, 99% percentiles: 0.01%, 0.1%, 1.2%).

We also study UDP over 5G. Since UDP does not provide congestion control, we manually increase the sending rate exponentially from 512 Kbps to 2 Gbps. we find that for sending rates up to 1 Gbps, the receiver-side loss rate is close to 0. This indicates 5G’s compatibility with UDP-based protocols such as QUIC [9] and HTTP/3 [4] at these low to medium data rates. However, at our test locations, **Verizon**’s 5G is not able to reliably sustain 2 Gbps or a higher sending rate over UDP, as we observe a packet loss rate of up to 17% at 2 Gbps.

## 4.2 Impact of the Environment

**Obstruction and NLoS Performance.** The experiments in §4.1 assume a clear LoS path without any obstruction. We now place different types of objects along the LoS path to test whether 5G signals can penetrate/bypass them. We first exemplify two most common obstructions: human body and hand. We stay at Location C (the Chicago hotel room) with an open window through which the phone has LoS to the

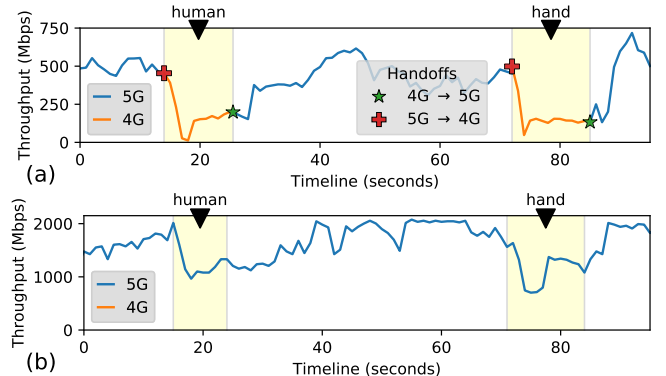


**Figure 3: Obstruction tests. (a) Location C with ineffective multipath, (b) Location A with effective multipath.**

5G-NR panel (62m). We launch a bulk transfer over 5G with 8 parallel TCP connections. During the data transfer, we block the LoS path by a human body and then a hand. We repeat the experiments for 10 times and observe qualitatively similar results, with one representative run illustrated in Figure 3(a). As shown, both obstructions trigger 5G-to-4G handoffs and lead to significant performance degradation. In contrast, when experimenting with 4G, neither blockage incurs noticeable throughput drop (figure not shown), due to the low-frequency bands used by 4G signals.

The above results show that it is difficult for 5G signals to penetrate a hand or human body, causing NLoS between the transmitter and receiver. We then study other types of obstructions using similar methods. We find that when the UE is inside a backpack, a cardboard box, or a clear glass, 5G signals can penetrate these containers (experimented with <100 meters distance to the 5G panel with LoS). However, 5G signals can hardly penetrate human body, trains, pillar structures, and tinted glass. We find that 5G works in vehicles since the front windshield is typically clear glass. However, when the vehicle is moving, mobility-incurred handoffs may considerably degrade 5G performance (§4.3).

We next repeat the same experiment in Location A, also using a human body and a hand as obstructions. As shown in Figure 3(b), the impact of the obstructions becomes smaller: the 5G connectivity persists despite a fair amount of performance degradation. Figures 3(a) and (b) indicate that the environment can affect the impact of obstructions. At Location A, despite the NLoS created by the obstructions, the nearby buildings can reflect signals and create multiple paths, and the reflected signal can still reach the UE. At Location C, the room has UV-protective windows that are very common in today’s buildings. Since the windows attenuate reflected 5G signals [43], multipath becomes ineffective. In other words, the only effective signal propagation path is through the open window. Blocking it inevitably degrades the performance.

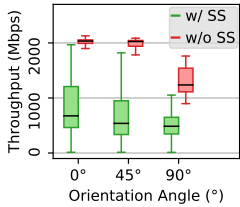


**Figure 4: Impact of UE-panel orientation.**

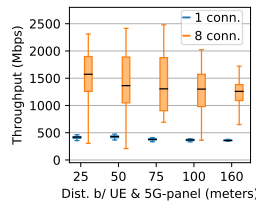


**Figure 5: Impact of UE-panel distance on throughput.**

**Impact of UE-panel Orientation.** We also investigate how the UE’s orientation to the panel affects network performance. We define the orientation as the minimum angle between the LoS and all normal vectors of the base station’s panels. As illustrated in Figure 2, an orientation of  $0^\circ$  is preferred because the panel is directly facing the UE, while an orientation of  $90^\circ$  is the least ideal case. Our orientation test is performed at Location D where we can find a large LoS area centered by a 5G tower. We pick three spots whose orientations are  $0^\circ$ ,  $45^\circ$ , and  $90^\circ$ . All spots have a 25m distance to the tower. At each spot, we perform three 60-second bulk download tests using 8 parallel connections. As shown in the “w/o SS” boxes in Figure 4 (the default setting of performing 60-second transfers excluding the slow start), we observe very small performance difference between  $0^\circ$  and  $45^\circ$  orientation, likely attributed to the environmental reflection and beamforming. However, in the extreme case where the orientation becomes  $90^\circ$ , we do observe a median throughput drop of 40%. The “w/ SS” boxes correspond to short (25-second) measurements from the very beginning of TCP connection establishment. They follow a similar trend except that when TCP slow start is considered, the throughput becomes lower.

**Impact of UE-Panel Distance.** We study how the distance between a UE and the panel affects network performance. We conduct the experiment at Location B, where we select five spots with their distances to the panel being 25m, 50m, 75m, 100m, and 160m, respectively. The panel and the five spots are on the same line. At each spot, we conduct three 60-second bulk download tests using 1 and 8 parallel TCP connection(s). During all tests, we ensure that the UE is always associated with the same panel, *i.e.*, there is no 5G-4G or 5G-5G handoff (§4.3). Our test location (B) makes this easy: recall that B is at the boundary of Minneapolis’ 5G coverage area; we can therefore increase the UE-panel distance by moving the UE away from the coverage area without worrying the UE connecting to a different panel. Achieving this inside the 5G coverage area is more difficult due to the dense deployment of 5G base stations. We find that at Location D (near the stadium), the phone can also reliably connect to the same panel at a long distance. So we conduct our test there as well.

Figure 5 plots the throughput distributions of different distances, where each box is across all 1-second samples measured at Locations B and D. As shown, the throughput only slightly reduces as the distance increases. For 8 parallel TCP connections, the median throughput decreases by only 17% (20%) at 100m (160m) compared to that at 25m. We attribute this to the clear LoS and sufficiently high transmission power of 5G antennas. For a single TCP connection, no noticeable throughput drop is observed because of the bandwidth under-utilization.

Overall, among all factors (obstruction, orientation, and distance), obstruction typically incurs the highest impact on 5G performance. Fortunately, in urban environments, surrounding signal reflections can oftentimes mitigate the performance degradation, allowing 5G to function under NLoS.

### 4.3 Handoffs in 5G

Handoffs in 5G differ from those in 4G/3G in both the horizontal and vertical dimensions. A Horizontal Handoff (HH) occurs when a UE’s association switches from one panel (in 5G’s term) to another. In 5G, HHs may frequently occur due to the smaller coverage of 5G panels compared to 4G towers. A Vertical Handoff (VH) is triggered when the wireless technology changes (*e.g.*, 5G to 4G). VHs are also prevalent in 5G whose signals are more unstable than 4G. Handoffs in 5G are more frequent than 4G due to small coverage of 5G base stations and the instability of 5G signals. 5G handoffs are also more complex as they involve switching between 4G and 5G subsystems.

We closely examine **Verizon**’s handoff mechanisms. In 5G NSA, a UE may be in one of the three states: (1) the UE is connected to 5G, (2) the UE is in 5G coverage area but is connected to 4G due to, for example, poor 5G signals, and (3) the UE is not in 5G area. We refer to these states as **C** (Connected to 5G), **R** (Ready for 5G but not yet connected), and **O** (outside 5G coverage), respectively, and we identify them by our monitoring tool. We use this state and the cell ID field (also collected by our tool) to track both HH and VH. Note that in 5G, cell IDs identify 5G-NR panels.

We then conduct experiments in both cities under various mobility levels (stationary, rotating, walking, and driving) to capture the above data related to handoffs. We identify 4 types of *primitive handoffs* ( $P_1$  to  $P_4$ ) as listed in the upper part of Table 2.  $P_1$  and  $P_2$  are VHs because there are handoffs between 4G and 5G. When a UE’s 5G signal strength drops (*e.g.*, due to an NLoS obstruction),  $P_1$  is triggered to downgrade the connectivity from 5G to 4G; when the network condition improves, the connectivity will be restored back to 5G ( $P_2$ ). Note that in the 5G-ready (R) mode, the UE actually connects to a 4G radio that is on the same tower (where the 5G-NR panel resides) or a nearby tower, but the cell ID does

Type	Description	Sequence
<i>P1</i>	VH, 5G→4G, same cellID	C1→R1
<i>P2</i>	VH, 4G→5G, same cellID	R1→C1
<i>P3</i>	VH+HH, 5G→4G, diff cellID	C1→R2
<i>P4</i>	HH, 4G→4G, diff cellID	R1→R2
Type	Description	Sequence
<i>O1</i>	5G temporarily disrupted, same panel	P1, P2
<i>O2</i>	5G to 5G between two panels	P3, P2
<i>O3</i>	5G to 5G between two panels	P1, P4, P2
<i>O4</i>	5G to 4G between two panels	P1, P4
<i>O5</i>	4G to 5G between two panels	P4, P2

Table 2: Primitive (top) & combinational (bottom) handoffs.

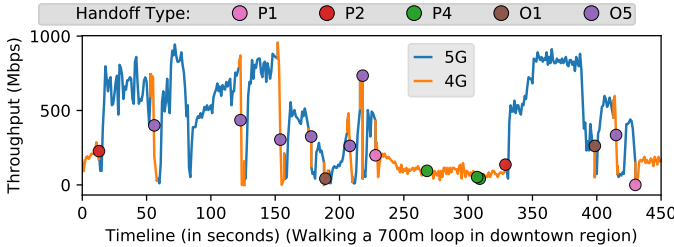


Figure 6: 5G throughput and handoffs under low mobility.

not change. This is likely because of NSA where 4G and 5G are deeply coupled. At the R state, the UE is still closely monitoring the original 5G panel for a possible 4G to 5G upgrade. *P3* is similar to *P1* except that the 5G to 4G downgrade ends at a different cell ID (panel). *P4* is a 4G to 4G HH from one cell ID to another. We do not observe a C1→C2 or R1→C2 sequence in our data. This is likely because NSA uses 4G for control-plane signaling – the UE will always first associate with the new cell’s 4G radio for control message exchanges before establishing the 5G data channel.

Interestingly, we also find that the (in)activity of user traffic can trigger 4G-5G handoffs. A *P1* handoff will occur when there is an inactivity of user traffic for ~10 seconds; at the R state, any user traffic will restore the 5G connectivity through a *P2* handoff, if the 5G signal is good. The rationale of such traffic-guided handoffs is possibly to reduce the 5G standby time that may consume additional energy.

From our data, we observe that oftentimes the primitive handoffs form complex sequences that we call *combinational handoff sequences*. We identify them by clustering primitive handoffs using an interval threshold (set to 10 seconds). They are exemplified at the bottom part of Table 2 as *O1* to *O5*. These combinational sequences correspond to high-level events that can not be realized by a single primitive handoff. For example, *O3* represents a 5G-to-5G handoff that consists of three primitive handoffs: a 5G to 4G VH on the old panel, a 4G to 4G HH from the old to new panel, and a 4G to 5G VH on the new panel. The whole procedure takes several seconds to finish.

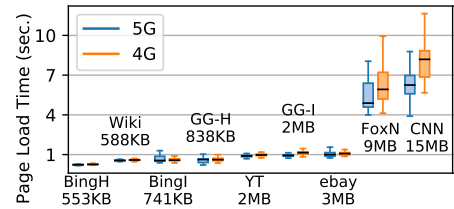
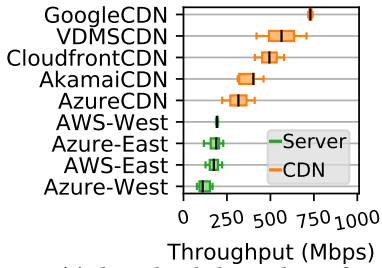


Figure 7: 4G/5G PLT over 9 pages: Bing, Wikipedia, Bing Search, Google, YouTube, Google Search, eBay, FoxNews, CNN.

We next show a case study to demonstrate the impact of handoffs. In this experiment, one of the authors holds a phone while walking at a normal speed (~5 km/h) at Location A for about 8 minutes. The phone keeps downloading data from a server over 8 parallel connections. Figure 6 plots the throughput, cellular connectivity (4G/5G), and handoffs. During this 8-minute walk, the phone experiences 31 primitive handoffs and bounces between 4G and 5G for 13 times. Such frequent switches make the throughput highly fluctuating, ranging from 0 to 954 Mbps. This may confuse applications (e.g., video rate adaptation logic [18, 22, 42]) and bring highly inconsistent user experiences. The above results highlight the need for cross-layer efforts that improve 5G performance under (even low) mobility. Some directions for example include PHY/MAC enhancements for reducing the handoff frequency, and robust upper-layer solutions that can adapt to frequent 4G/5G handoffs, such as MPTCP [24] and prefetching [13].

#### 4.4 Application Performance

**Web Browsing.** We develop a WebView-based browser and use it to programmatically load the landing pages of 9 popular websites listed in Figure 7 over 5G and 4G. We then compare their page loading time (PLT). We conduct the experiments at Locations A and C with SGS10 (5G) and SGS9 (4G). In order to make a fair comparison, we confirm that both devices yield statistically similar PLT when loading diverse web pages *locally*. In Location A (C), the UE-panel distance is 50m (62m) with LoS. For each site, We use an automated script to perform cold-cache loading (*i.e.*, with an empty web cache) over 5G and 4G back-to-back, and repeat this for 30 times. As shown in Figure 7, for most sites with small page sizes ( $\leq 3$  MB), 4G and 5G achieve similar PLT. This is attributed to two reasons. First, web browsing requires a synergy between network transfer and local processing, with the latter oftentimes being the bottleneck in particular for small web pages [40]. Second, as we load the pages from the original content providers, the bottleneck may shift from the wireless hop to the Internet. For large pages (FoxNews and CNN), loading them over 5G does shorten the median PLT by 17.5% and 23.6%, respectively, because of the reduction of the content fetch time.



**Figure 8: HTTP(S) download throughput for 9 CDN/cloud servers over 5G.**

**HTTP(S) Download.** We investigate the HTTP(S) download performance. We upload a 1GB file to geographically distributed public cloud instances and CDN servers<sup>2</sup>. We then develop a custom HTTP(S) client that issues 8 parallel byte-range requests each fetching 1/8 of the file over 5G. The experiments are conducted at Locations A and C (clear LoS with a UE-panel distance of 30m for A and 62m for C, 0° orientation). For each server, we repeat the file download for 3 times at both locations, and measure the average throughput.

The results are shown in Figure 8. We find that all cloud/CDN servers exhibit low throughput compared to the **iPerf** throughput shown in Figure 1(a): the average throughput ranges from 119 to 730 Mbps with a median of 222 Mbps across all servers. The somewhat surprising results make us realize that HTTP(S) download is very different from **iPerf** bandwidth probing. Multiple factors may slow down HTTP(S) download, such as the HTTP request latency, TCP slow start, DNS time, Internet-side bottleneck link, server-side data processing (e.g., HTTP chunked mode and HTTP/2 multiplexing), HTTPS encryption/decryption, unbalanced byte-range sessions (some sessions may finish earlier than others [10]), to name a few. Although these factors already exist in 3G/4G eras, they are *amplified* in 5G due to its high speed. The above results indicate that 5G’s high throughput does not always translate to better app QoE, whose improvement requires joint, cross-layer optimizations from multiple sources.

## 5 CONCLUDING REMARKS

Our study on the world’s first commercial mmWave 5G network quantitatively reveal 5G performance on COTS smartphones to the community. Our study identifies key research directions on improving 5G users’ experience in a cross-layer manner. For example, how to design 5G-friendly transport protocols? How to strategically select interface(s) among 5G, 4G, and WiFi? What type of support should a mobile OS provide for enhancing QoE over 5G? Meanwhile, we admit that this short paper leaves many interesting measurement questions unanswered, such as 5G video streaming performance, interaction between 5G and various TCP congestion control schemes, and detailed 5G radio energy models. We

<sup>2</sup> We do not use the CDN servers to perform most measurements in early sections because we could not run **iPerf** on these servers.

plan to explore them in our future work. Finally, we did not address 5G upload performance because **Verizon**’s mmWave deployment did not support high upload speeds, the highest we achieved was 60Mbps.

**Acknowledgement.** This research was supported in part by NSF under Grants CNS-1618339, CNS-1617729, CNS-1814322, CNS-1831140, CNS-1836772, and CNS-1901103.

## REFERENCES

- [1] Omid Abari, Dinesh Bharadia, Austin Duffield, and Dina Katabi. 2017. Enabling high-quality untethered virtual reality. In *Proceedings of the 14th USENIX Symposium on Networked Systems Design and Implementation*. 531–544.
- [2] Christopher R Anderson and Theodore S Rappaport. 2004. In-building wideband partition loss measurements at 2.5 and 60 GHz. *IEEE transactions on wireless communications* 3, 3 (2004), 922–928.
- [3] M. Belshe, R. Peon, and Ed. M. Thomson. 2015. *Hypertext Transfer Protocol Version 2 (HTTP/2)*. RFC 7540. Internet Engineering Task Force. <https://tools.ietf.org/html/rfc7540>
- [4] Mike Bishop. 2019. Hypertext Transfer Protocol Version 3 (HTTP/3) (IETF Draft). (2019). Retrieved June 2019 from <https://quicwg.org/base-drafts/draft-ietf-quic-http.html>
- [5] Sylvain Collonge, Gheorghe Zaharia, and G EL Zein. 2004. Influence of the human activity on wide-band characteristics of the 60 GHz indoor radio channel. *IEEE Transactions on Wireless Communications* 3, 6 (2004), 2396–2406.
- [6] Haotian Deng, Chunyi Peng, Ans Fida, Jiayi Meng, and Y Charlie Hu. 2018. Mobility Support in Cellular Networks: A Measurement Study on Its Configurations and Implications. In *Proceedings of the Internet Measurement Conference 2018*. ACM, 147–160.
- [7] Leica Geosystems. 2019. Leica DISTO E7500i LDM. (June 2019). Retrieved June 2019 from <https://lasers.leica-geosystems.com/disto/e7500i>
- [8] Marco Giordani, Marco Mezzavilla, and Michele Zorzi. 2016. Initial Access in 5G mmWave Cellular Networks. *IEEE Communications Magazine* 54, 11 (2016), 40–47.
- [9] Google. 2019. QUIC, a multiplexed stream transport over UDP. (2019). Retrieved June 2019 from <https://www.chromium.org/quic>
- [10] Yihua Ethan Guo, Ashkan Nikravesh, Z Morley Mao, Feng Qian, and Subhabrata Sen. 2017. Accelerating multipath transport through balanced subflow completion. In *Proceedings of the 23rd Annual International Conference on Mobile Computing and Networking*. ACM, 141–153.
- [11] Muhammad Kumail Haider, Yasaman Ghasempour, Dimitrios Koutsikolas, and Edward W Knightly. 2018. Lister: mmwave beam acquisition and steering by tracking indicator leds on wireless aps. In *Proceedings of the 24th Annual International Conference on Mobile Computing and Networking*. ACM, 273–288.
- [12] Daniel Halperin, Srikanth Kandula, Jitendra Padhye, Paramvir Bahl, and David Wetherall. 2011. Augmenting data center networks with multi-gigabit wireless links. In *ACM SIGCOMM Computer Communication Review*, Vol. 41. ACM, 38–49.
- [13] Brett D Higgins, Jason Flinn, Thomas J Giuli, Brian Noble, Christopher Peplin, and David Watson. 2012. Informed mobile prefetching. In *Proceedings of the 10th international conference on Mobile systems, applications, and services*. ACM, 155–168.
- [14] Anders Hillbur. 2018. 5G deployment options to reduce the complexity. (November 2018). Retrieved June 2019 from <https://www.ericsson.com/en/blog/2018/11/5g-deployment-options-to-reduce-the-complexity>
- [15] Junxian Huang, Feng Qian, Yihua Guo, Yuanyuan Zhou, Qiang Xu, Z Morley Mao, Subhabrata Sen, and Oliver Spatscheck. 2013. An in-depth study of LTE: effect of network protocol and application

behavior on performance. In *ACM SIGCOMM*.

[16] Junxian Huang, Qiang Xu, Birjodh Tiwana, Z Morley Mao, Ming Zhang, and Paramvir Bahl. 2010. Anatomizing application performance differences on smartphones. In *Proceedings of the 8th international conference on Mobile systems, applications, and services*. ACM, 165–178.

[17] Haiqing Jiang, Yaogong Wang, Kyunghan Lee, and Injong Rhee. 2012. Tackling bufferbloat in 3G/4G networks. In *Proceedings of the 2012 Internet Measurement Conference*. ACM, 329–342.

[18] Junchen Jiang, Vyas Sekar, and Hui Zhang. 2012. Improving Fairness, Efficiency, and Stability in HTTP-Based Adaptive Video Streaming With Festive. In *Proceedings of CoNEXT 2012*. ACM, 97–108.

[19] ESnet/Lawrence Berkeley National Laboratory. 2019. iperf3: A TCP, UDP, and SCTP network bandwidth measurement tool. (June 2019). Retrieved June 2019 from <https://github.com/esnet/iperf/releases/tag/3.6>

[20] Li Li, Ke Xu, Tong Li, Kai Zheng, Chunyi Peng, Dan Wang, Xiangxiang Wang, Meng Shen, and Rashid Mijumbi. 2018. A measurement study on multi-path TCP with multiple cellular carriers on high speed rails. In *Proceedings of the 2018 Conference of the ACM Special Interest Group on Data Communication*. ACM, 161–175.

[21] Yuanjie Li, Chunyi Peng, Zengwen Yuan, Jiayao Li, Haotian Deng, and Tao Wang. 2016. Mobileinsight: Extracting and analyzing cellular network information on smartphones. In *Proceedings of the 22nd Annual International Conference on Mobile Computing and Networking*. ACM.

[22] Hongzi Mao, Ravi Netravali, and Mohammad Alizadeh. 2017. Neural adaptive video streaming with pensieve. In *Proceedings of the Conference of the ACM Special Interest Group on Data Communication*. ACM, 197–210.

[23] Motorola. 2019. 5G Moto Mod. (2019). Retrieved June 2019 from <https://www.motorola.com/us/products/moto-mods/moto-5g>

[24] Ashkan Nikravesh, Yihua Guo, Feng Qian, Z Morley Mao, and Subhabrata Sen. 2016. An in-depth understanding of multipath TCP on mobile devices: measurement and system design. In *Proceedings of the 22nd Annual International Conference on Mobile Computing and Networking*. ACM, 189–201.

[25] Thomas Nitsche, Guillermo Bielsa, Irene Tejado, Adrian Loch, and Joerg Widmer. 2015. Boon and bane of 60 GHz networks: practical insights into beamforming, interference, and frame level operation. In *Proceedings of the 11th ACM Conference on Emerging Networking Experiments and Technologies*. ACM, 17.

[26] Thomas Nitsche, Adriana B Flores, Edward W Knightly, and Joerg Widmer. 2015. Steering with eyes closed: mm-wave beam steering without in-band measurement. In *Computer Communications (INFOCOM), 2015 IEEE Conference on*. IEEE, 2416–2424.

[27] Joan Palacios, Danilo De Donno, and Joerg Widmer. 2017. Tracking mm-Wave channel dynamics: Fast beam training strategies under mobility. In *Proceedings of the IEEE Conference on Computer Communications*.

[28] Hang Qiu, Fawad Ahmad, Fan Bai, Marco Gruteser, and Ramesh Govindan. 2018. AVR: Augmented Vehicular Reality. In *Proceedings of the 16th Annual International Conference on Mobile Systems, Applications, and Services*. ACM, 81–95.

[29] Qualcomm. 2019. Everything You Need to Know About 5G. (2019). Retrieved June 2019 from <https://www.qualcomm.com/invention/5g/what-is-5g>

[30] Qualcomm. 2019. Mobilizing mmWave for smartphones. (2019). Retrieved June 2019 from <https://www.qualcomm.com/news/onq/2019/02/13/track-solve-another-impossible-challenge-mobilizing-mmwave-smartphones>

[31] Theodore S Rappaport, Eshar Ben-Dor, James N Murdock, and Yijun Qiao. 2012. 38 GHz and 60 GHz angle-dependent propagation for cellular & peer-to-peer wireless communications. In *Communications (ICC), 2012 IEEE International Conference on*. IEEE, 4568–4573.

[32] Theodore S Rappaport, Felix Gutierrez, Eshar Ben-Dor, James N Murdock, Yijun Qiao, and Jonathan I Tamir. 2013. Broadband millimeter-wave propagation measurements and models using adaptive-beam antennas for outdoor urban cellular communications. *IEEE transactions on antennas and propagation* 61, 4 (2013), 1850–1859.

[33] Theodore S Rappaport, Shu Sun, Rimma Mayzus, Hang Zhao, Yaniv Azar, Kevin Wang, George N Wong, Jocelyn K Schulz, Mathew Samimi, and Felix Gutierrez. 2013. Millimeter wave mobile communications for 5G cellular: It will work! *IEEE access* 1 (2013), 335–349.

[34] Wonil Roh, Ji-Yun Seol, Jeongho Park, Byunghwan Lee, Jaekon Lee, Yungsoo Kim, Jaeweon Cho, Kyungwhoon Cheun, and Farshid Aryanfar. 2014. Millimeter-wave beamforming as an enabling technology for 5G cellular communications: theoretical feasibility and prototype results. *IEEE Communications Magazine* 52, 2 (2014), 106–113.

[35] Clayton Shepard, Ahmad Rahmati, Chad Tossell, Lin Zhong, and Phillip Kortum. 2011. LiveLab: measuring wireless networks and smartphone users in the field. *ACM SIGMETRICS Performance Evaluation Review* 38, 3 (2011), 15–20.

[36] Sanjib Sur, Ioannis Pefkianakis, Xinyu Zhang, and Kyu-Han Kim. 2017. WiFi-Assisted 60 GHz Wireless Networks. In *MobiCom*.

[37] Sanjib Sur, Vignesh Venkateswaran, Xinyu Zhang, and Parmesh Ramanathan. 2015. 60 ghz indoor networking through flexible beams: A link-level profiling. In *ACM SIGMETRICS Performance Evaluation Review*, Vol. 43. ACM, 71–84.

[38] Zhaowei Tan, Yuanjie Li, Qianru Li, Zhehui Zhang, Zhehan Li, and Songwu Lu. 2018. Supporting mobile VR in LTE networks: How close are we? *Proceedings of the ACM on Measurement and Analysis of Computing Systems* 2, 1 (2018), 8.

[39] Xiaozheng Tie, Kishore Ramachandran, and Rajesh Mahindra. 2012. On 60 ghz wireless link performance in indoor environments. In *Passive and Active Measurement*. Springer, 147–157.

[40] Xiao Sophia Wang, Aruna Balasubramanian, Arvind Krishnamurthy, and David Wetherall. 2013. Demystifying page load performance with WProf. In *Presented as part of the 10th {USENIX} Symposium on Networked Systems Design and Implementation ({NSDI} 13)*. 473–485.

[41] Hao Xu, Vikas Kukshya, and Theodore S Rappaport. 2002. Spatial and temporal characteristics of 60-GHz indoor channels. *IEEE Journal on selected areas in communications* 20, 3 (2002), 620–630.

[42] Xiaoqi Yin, Abhishek Jindal, Vyas Sekar, and Bruno Sinopoli. 2015. A control-theoretic approach for dynamic adaptive video streaming over HTTP. In *ACM SIGCOMM Computer Communication Review*, Vol. 45. ACM, 325–338.

[43] Hang Zhao, Rimma Mayzus, Shu Sun, Mathew Samimi, Jocelyn K Schulz, Yaniv Azar, Kevin Wang, George N Wong, Felix Gutierrez Jr, and Theodore S Rappaport. 2013. 28 GHz millimeter wave cellular communication measurements for reflection and penetration loss in and around buildings in New York city. In *ICC*. 5163–5167.

[44] Xia Zhou, Zengbin Zhang, Yibo Zhu, Yubo Li, Saipriya Kumar, Amin Vahdat, Ben Y Zhao, and Haitao Zheng. 2012. Mirror mirror on the ceiling: Flexible wireless links for data centers. *ACM SIGCOMM Computer Communication Review* 42, 4 (2012), 443–454.

[45] Yibo Zhu, Zengbin Zhang, Zhinus Marzi, Chris Nelson, Upamanyu Madhow, Ben Y Zhao, and Haitao Zheng. 2014. Demystifying 60GHz outdoor picocells. In *Proceedings of the 20th annual international conference on Mobile computing and networking*. ACM, 5–16.

[46] Yibo Zhu, Xia Zhou, Zengbin Zhang, Lin Zhou, Amin Vahdat, Ben Y Zhao, and Haitao Zheng. 2014. Cutting the cord: a robust wireless facilities network for data centers. In *Proceedings of the 20th annual international conference on Mobile computing and networking*. ACM, 581–592.